

## Hybrid Microwave-DC Discharge in Nitrogen at Reduced Pressures

Yu. A. Lebedev<sup>a,\*</sup>, G. V. Krashevskaya<sup>a,b</sup>, A. Yu. Titov<sup>a</sup>, and I. L. Epstein<sup>a</sup>

<sup>a</sup>Topchiev Institute of Petrochemical Synthesis of the Russian Academy of Sciences (TIPS RAS), Moscow, 119991 Russia

<sup>b</sup>National Nuclear Research University MEPhI, Moscow, 115409 Russia

\*e-mail: lebedev@ips.ac.ru

Received February 28, 2019; revised February 28, 2019; accepted May 16, 2019

**Abstract**—The hybrid nonuniform microwave-DC discharge in nitrogen at pressure 1–15 Torr is studied by the method optical emission spectroscopy with spatial resolution. Discharge is ignited between the microwave powered antenna and grounded disk electrode placed at the distance of 2.5 cm from antenna. Antenna was positively biased relative to the grounded electrode. The ratio of the intensities of the nitrogen band at 337 nm and the emission of the ion band at 391 nm is used to determine the microwave field strength. Second positive system of nitrogen emission prevails over others in near antenna region. Emission of the first negative nitrogen ion system has the highest intensity near flat electrode. The vibrational distributions of nitrogen molecules and their dependence on direct current and position between antenna and grounded electrode are determined.

DOI: 10.1134/S0018151X19050109

### INTRODUCTION

The main directions of development of work on the physics of low-temperature plasma and its application are described in the 2012 and 2017 road maps [1, 2]. Realization of these directions is hardly possible without solving the problem of controlling the parameters of a nonequilibrium low-temperature plasma. Traditional methods are changing the external parameters of electric discharges (energy input and pressure, plasma gas composition, introduction of small additives that change the ionization mechanism, etc.). A promising direction is the use of hybrid discharges. Their use is effective if it is necessary to enhance the positive properties of one of the discharges, to provide the conditions necessary for the realization of particular process and unattainable in one discharge, if it is necessary to obtain a discharge at power levels insufficient to maintain the discharge, to change the discharge geometry, etc.

Hybrid discharges have a long history and some examples are given below.

External magnetic fields are used to improve the matching of the discharge device with a microwave generator [3]. Inhomogeneous magnetic fields cause plasma acceleration and transport of plasma particles in the direction of a decreasing field [4]. This is used to intensify the effects of plasma on the treated samples [5–7]. Magnetic fields make it possible to protect the walls of the reactor and the dielectric windows from plasma exposure [8]. To obtain plasma in large volumes, plasma is used in a multipole environment [9]. Reducing the loss of charged particles on the walls

allows to reduce the intensity of the microwave field, necessary to maintain the discharge.

Articles [10, 11] described hybrid microwave-RF systems in which plasma was created by a microwave source, and the RF field provided a DC displacement of the substrate during its processing.

The use of DC fields allows, depending on the polarity, both to increase and decrease the threshold for the appearance of a multipactor discharge near the surface of the dielectric [12].

Possibilities of controlling the parameters of an RF discharge using an external magnetic field and introducing an additional DC electrode are described in [13]. Hybrid plasma torch, which is a combination of RF plasma torch and arc plasma torch is described in [14]. In [15], a plasma torch was described, which uses a combination of arc and microwave discharge. Combination of microwave plasma torch and AC high-voltage discharge plasma provides conditions for effective plasma sterilization [16]. Hybrid ECR-RF plasma device for etching is described in [17]. Hybrid helicon-ECR plasma source was described in [18]. The design of the system for thin film technology, which combines magnetron, arc and magnetic-activated inductive RF discharges is proposed in [19]. Gas temperature profile can be controlled in the hybrid microwave-plasma hot-wall reactor for synthesis of silica nanoparticles [20].

Thus, hybrid discharges make it possible to control the parameters of the plasma and change its characteristics.

Although a large number of discharge devices have been developed for producing microwave plasma for

solving many practical problems [21], it follows from a brief review that hybrid systems are also created based on microwave discharges.

This work describes the study of a hybrid microwave-DC discharge in nitrogen that arises when DC electric voltage, exceeding the threshold, is applied between a powered microwave antenna and a disk grounded electrode at reduced pressures.

When a DC voltage is applied between the antenna and the electrode, two cases are possible. In the first case, at voltages lower than a certain threshold, an additional discharge does not occur in the interelectrode gap, and the system can be considered as a microwave discharge immersed in the external DC field. The case of microwave discharge near antenna in nitrogen in the external DC field was studied in [22–24]. When DC voltage exceeds the threshold, the situation changes fundamentally. A DC discharge occurs in the gap and two discharges coexist in the gap: a microwave discharge and a direct current discharge. DC discharge disappears when microwave discharge is turned off. Combination of microwave and DC discharge is a hybrid microwave-DC discharge. This situation has not been previously considered and is the subject of this article.

Hybrid discharge is characterized by studying the axial distribution of the intensity of the discharge light emission in the space between the antenna and a disc grounded electrode.

## EXPERIMENTAL SETUP AND METHODS OF DIAGNOSTICS

Experiments were carried out on an installation described in detail in [23, 24] (Fig. 1). The discharge chamber is a stainless steel cylinder with a diameter of 15 cm, with four windows for discharge observation, located in a cylindrical wall. An electromagnetic wave (2.45 GHz) with a power varied within the limits of 60–100 W was fed into the discharge chamber through a waveguide-to-coaxial junction, the 5 mm diameter copper central conductor of which was prolonged in the discharge chamber and serves the microwave antenna. It is introduced into the chamber through the

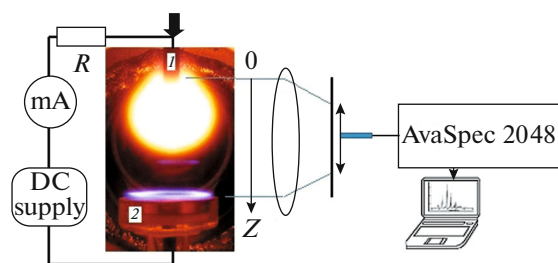


**Fig. 1.** Schematic of experimental setup: (1) antenna, (2) grounded electrode. Photograph corresponds to the pressure of 5 Torr, incident power of 100 W, DC current of 13 mA.

upper cup of the cylindrical chamber along the axis (discharge axis) through the vacuum seal. A grounded plane copper disk electrode with a diameter of 2.5 cm is placed below antenna at a distance of 25 mm from its end. Lateral surface of this electrode was covered with quartz. The antenna is isolated from the grounded chamber by DC. It allows changing independently the DC potential of antenna relative to the chamber and disk electrode. The DC voltage between the antenna and the electrode was varied from  $-200$  to  $+350$  V (the ballast resistor  $R$  was of 8 kOhm). The negative potential of the antenna had almost no effect on the microwave discharge [23, 24]. This paper presents results with positively biased antenna when applied DC voltage is sufficient for ignition of DC discharge in the gap between the powered antenna and grounded electrode, i.e. sufficient for creation of hybrid microwave-DC discharge. All results presented below were obtained in the regime of hybrid discharge.

The discharge camera is equipped with quartz windows to observe the discharge. The microwave discharge is ignited near the end of the antenna. The luminous region of the discharge have a radially symmetric structure with a bright near-electrode region (region of self-sustained discharge) and a spherical outer region with a sharp boundary (region of a non-self-sustaining discharge). The region occupied by the luminous plasma is much smaller than the distance between antenna and disc electrode. For visualization of the discharge (spatial distributions of the spectral radiation intensity of the discharge and along the line of sight) and for investigation of emission spectra in the 200–700 nm range, the unit is equipped with a nanosecond electron-optical video camera K-008, operating in a continuous recording mode and with AvaSpec-2048 spectrometer (spectral resolution was of 1 nm). A quartz condenser projected a plasma image to the plane of the input aperture of the movable optical fiber. The fiber could move in the axial direction from the end of antenna to the grounded electrode giving the spatial distribution of plasma emission (the spatial resolution of the system was not worse than 0.1 mm).

Experiments were carried out in nitrogen at pressures of 1–15 Torr and nitrogen flow rate of 60 sccm. The main results of optical emission spectroscopy were obtained at pressures of 1–9 Torr. Nitrogen was fed through a channel in the top chamber cover. The MKS system, consisting of a controlled flowmeter, a throttling tap and a capacitive pressure meter (Baratron), was used for independent control of pressure and gas flow.

## RESULTS AND DISCUSSION

Figure 2 shows an example of the emission spectrum of a hybrid discharge in the vicinity of an antenna and near the grounded disk electrode. Antenna was positively biased against the grounded electrode. It

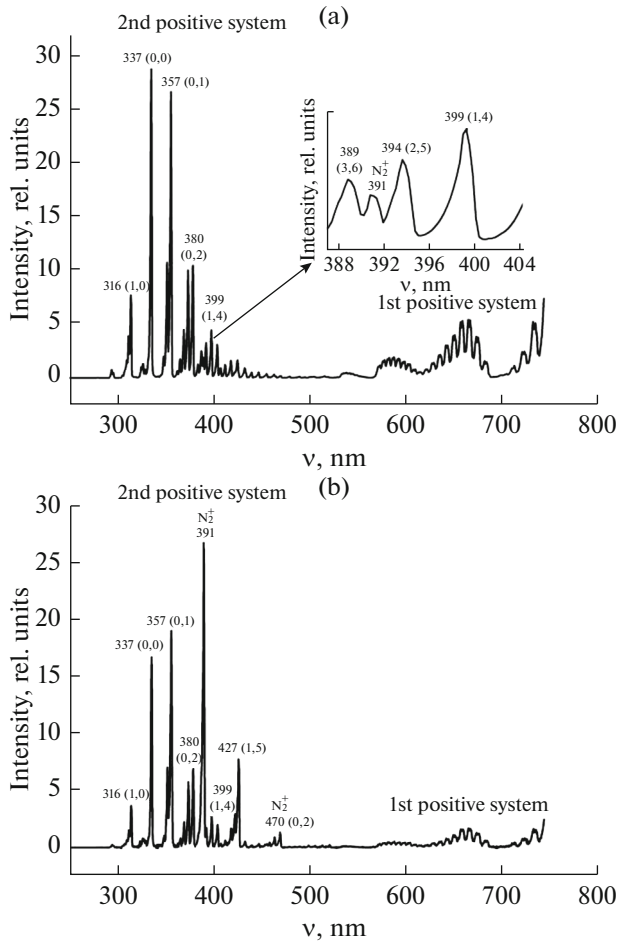


**Fig. 2.** Optical emission spectra of hybrid discharge at pressure 1 Torr and DC current 4 mA: (a) region near antenna, (b) region near disk electrode (intensities of emission spectra in the region near a disk electrode was increased by a factor of 6).

can be seen that the radiation is represented by the bands of the first (FPS)  $N_2(B^3\Pi_g \rightarrow A^3\Sigma_u^+)$  and second (SPS) positive  $N_2(C^3\Pi_u \rightarrow B^3\Pi_g)$  nitrogen sys-

tems, as well as the first negative system (FNS) of  $N_2^+(B^2\Sigma_u^+ \rightarrow X^2\Sigma_g^+)$  nitrogen ion [25].

It is seen that the spectra are fundamentally different. Near the antenna in the short-wave length region of the spectrum the emission of SPS bands dominates, and near the disk electrode the emission of FNS bands dominates. The spectra of Fig. 2 are consistent with those given in [26] for the anode and cathode regions of a DC discharge. Since the antenna is positively biased relative to the disk electrode, the latter plays the role of a cathode in the discharge system under consideration. This is confirmed by the photographs (Fig. 3) showing the change in the discharge area near the electrode from DC current. It can be seen that the discharge exists in the mode of normal cathode fall and the area covered by the discharge depends on the discharge current.

Since the microwave discharge near antenna plays an important role in the considered discharge system, before proceeding to presenting further results, we briefly summarize the known information about the properties and parameters of the discharge at the antenna without applying a DC voltage [27–31].

Microwave discharge is concentrated near the antenna and visible size of it is less than the distance between the antenna and the disk electrode. The microwave discharge is an inhomogeneous plasma formation with the main energy absorption region located in a thin near-surface plasma layer.

The discharge has a non-uniform structure consisting of two areas: a bright thin ( $\sim 1$  mm) plasma layer at the antenna and a spherical halo surrounding it (Fig. 1). With increasing pressure, the halo decreases and disappears (the trend is clear from comparison of Figs. 1 and 3).

The plasma layer is a self-sustaining microwave discharge region with electron concentration of the order of  $1.5 \times 10^{11} \text{ cm}^{-3}$ , exceeding the critical concentration for a microwave field frequency of 2.45 GHz ( $n_c \sim 7.45 \times 10^{10} \text{ cm}^{-3}$ ). In this area, the conditions for

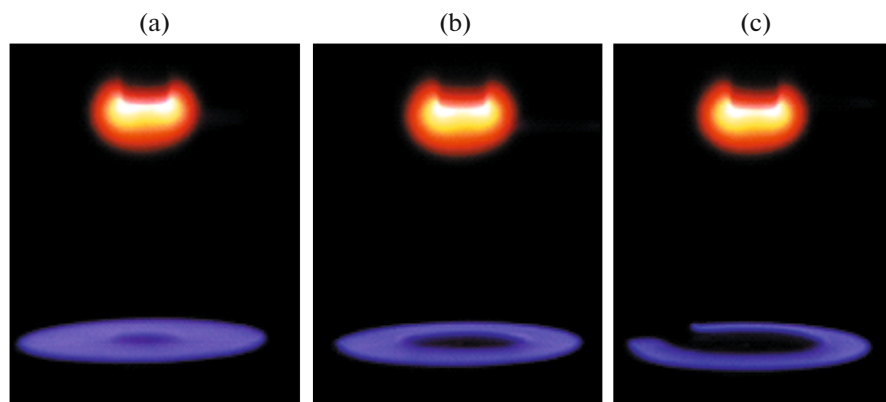


**Fig. 3.** Photos of discharge at pressure 14.5 Torr and incident microwave power 80 W: (a) DC current of 30 mA, (b) 25 mA, and (c) 17 mA.

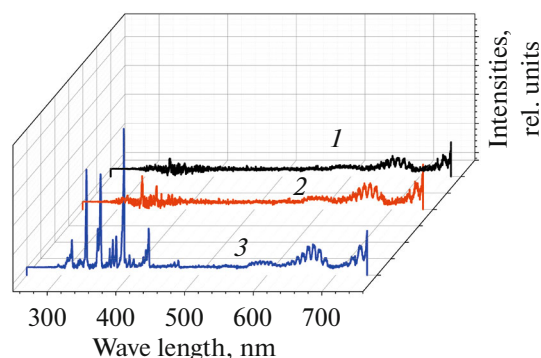


**Fig. 4.** Optical emission spectra against DC current in the region near the flat grounded electrode: (1) 0 mA, (2) 0.6 mA, and (3) 6 mA.

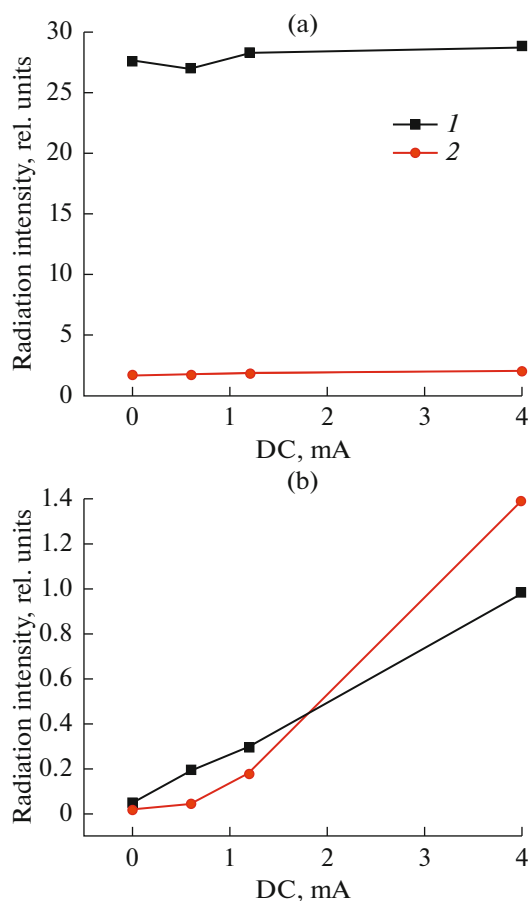


**Fig. 5.** Intensities of emission of nitrogen and nitrogen ion bands against DC current at pressure 1 Torr: (a) region near antenna, (b) region near the disk electrode; (1) 337 nm and (2) 391 nm.

the existence of plasma resonance are realized, there are significant electric fields and electron impact is predominant in the processes of excitation of electronic states of molecules. The main energy input to the microwave plasma occurs in this layer. The main ion in this region is  $N_2^+$  ion.

In the halo the electric fields and electron concentrations are much smaller, and processes involving electron-excited particles ( $N_2(A^3\Sigma_u^+)$ ,  $N_2(a^1\Sigma_u^-)$ ,  $N(^2D)$ ,  $N(^2P)$ ) dominate in the processes of excitation. This area is the area of non-self-sustained discharge. Excited particles and atoms can come here from the plasma layer at the antenna as a result of diffusion. Such a difference in the mechanisms of the processes is also reflected in the spectral composition of the discharge radiation: in the antenna layer, the emission of the second positive (SPS) nitrogen system dominates, whereas in halo the emission of the first positive (FPS) nitrogen system plays a major role.

The rotational temperature  $T_{rot}$  of nitrogen determined by SPS radiation and averaged over the line of view perpendicular to the discharge axis lies within 500–1100 K in the range of incident microwave powers between 30 and 110 W and pressures of 1–16 Torr.

It follows from all the above that the microwave discharge provides the pre-activation of the discharge gap of the hybrid discharge and the DC discharge is created in an environment with excited and charged particles. This facilitates the conditions of occurrence of the discharge, and allows one to control its properties by changing the incident microwave power. The fact of the presence of excited molecules in the region and a grounded electrode is confirmed by the registration of FPS radiation in it without applying a DC voltage (Fig. 4).

When DC voltage is applied to the interelectrode gap between antenna with microwave plasma and disk electrode it is necessary to take into account the following (this problem was considered in details in [22] for the case of DC voltage insufficient for ignition of hybrid discharge).

The distribution of the DC voltage in the gap is non-uniform, and it is in accordance with the distribution of conductivity of the gap. Since there is plasma with high electron concentration in the antenna area, the conductivity of this area is much larger than the conductivity of the rest of the gap, and the DC voltage drop in it is small. This means that almost all applied voltage is concentrated in the area of the disk electrode (at voltage sufficient for DC discharge ignition the glow appeared near the disk electrode indicating the creation of the hybrid discharge). This also means that the influence of DC voltage on the plasma area at the antenna is small (Fig. 5a) and change in the properties of this area (e.g., change in the incident microwave power) gives an independent channel of control for the properties of the hybrid discharge. There is large dependence of plasma properties on DC current in the region near the disk electrode (Fig. 5b). Distributions of the second positive and first negative bands emissions in the gap are shown in Fig. 6.

Figure 7 shows that vibrational distribution of nitrogen molecules in the  $C^3\Pi_u$  state near the antenna

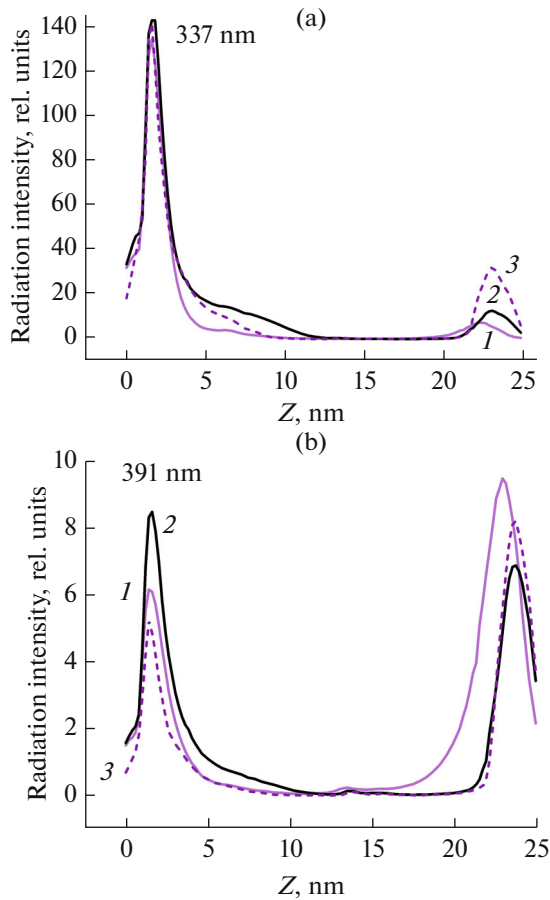


**Fig. 6.** Axial distributions of the second positive (a) and first negative (b) bands of nitrogen emission in the inter-electrode gap at pressures of 2 (1), 5 (2), and 9 (3) Torr and DC current of 6 mA.

differs from Boltzmann distribution and weakly dependent on the direct current (Fig. 7a). The vibrational distribution of nitrogen molecules in the  $C^3\Pi_u$  state near the grounded electrode is not Boltzmann, the excitation temperature of the first level is lower than that in the antenna region and increases with increasing DC current (Fig. 7b). The ratio of excitation temperatures of the first vibrational level of  $C^3\Pi_u$  state near antenna ( $T_{\text{ex1A}}$ ) and near the grounded electrode ( $T_{\text{ex1E}}$ ) is of 2 at DC current of 1.2 mA and decreases to 1.4 with increasing current (4 mA). Differences of temperatures decreases with increasing pressure.

The microwave field strength near the antenna can be determined from comparison of measured and calculated ratios of intensities of the second positive and first negative bands of nitrogen [24]. This method can be used if excitation of radiative states is provided by the electron impact and its deactivation is the result of light emission. These conditions are realized in the plasma layer near antenna. The Boltzmann equation for a stationary, isotropic part of the electron energy

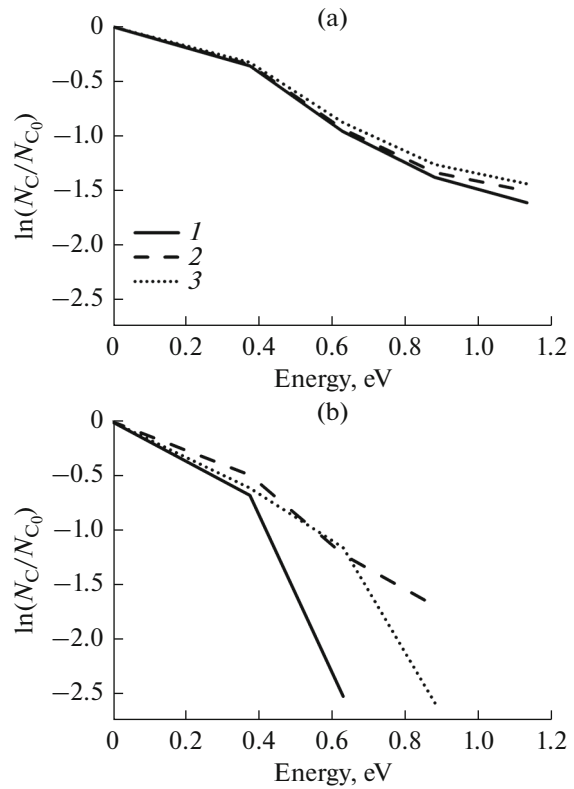


**Fig. 7.** Vibrational distributions of nitrogen molecules in the state  $N_2(C^3\Pi_u)$  in the region near antenna (a) and near the disk electrode (b); curves are normalized to the concentration of molecules on the zero level  $N_{C_0}$ ; (1) 1 Torr and 1.2 mA, (2) 1 Torr and 4 mA, and (3) 2 Torr and 1.2 mA.

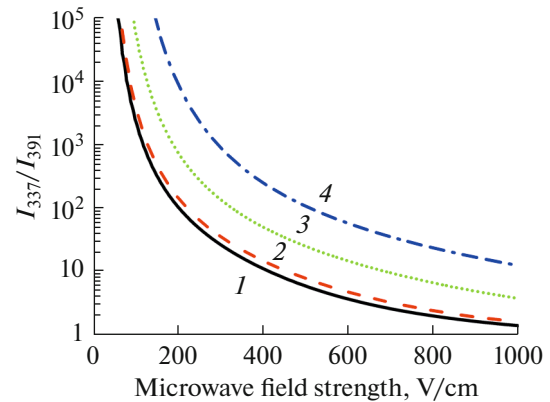


**Fig. 8.** Calculated dependences of the ratio of emission intensities of nitrogen at wavelengths 337 and 391 nm on the microwave field at gas temperature of 600 K and different pressures: (1) 1 Torr, (2) 2 Torr, (3) 3 Torr, and (4) 4 Torr.

distribution function (EEDF), recorded in the two-term approximation of the EEDF expansion into spherical harmonics has been used for calculations the ratios of emission intensities. The emission bands of the second positive system of nitrogen at 337 nm and



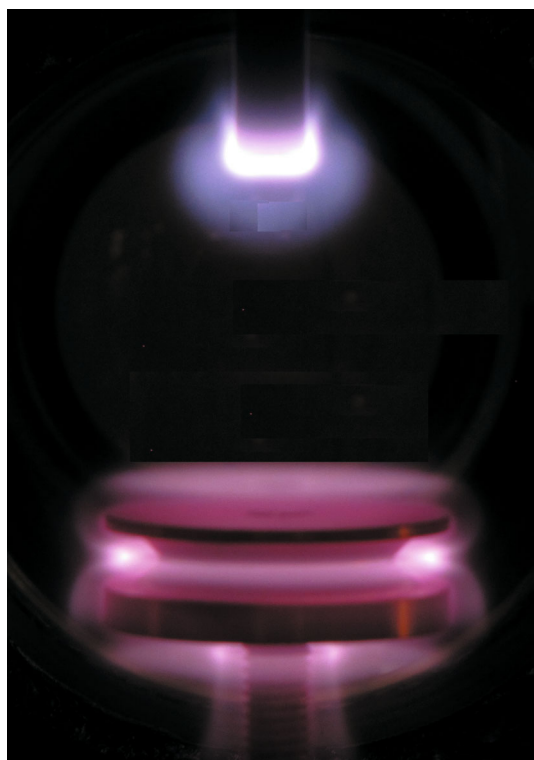


**Fig. 9.** Hybrid microwave-DC discharge with complex shape electrode.

the first negative system of nitrogen ion at 391 nm were calculated. Results are shown in Fig. 8. It was shown that the value of microwave field does not depend on the DC current. Peak values of the field increases with pressure and lies in the interval 410–880 V/cm at pressures of 1–9 Torr.

The hybrid discharge described above can be used to solve various applied problems: plasma treatment (cleaning, modification, etching, film deposition) of internal surfaces of large chambers and surface plasma treatment of parts of complex shape. Example of the latter case is shown in Fig. 9.

### CONCLUSIONS

Method optical emission spectroscopy was used to characterize the properties of the hybrid microwave-DC discharge in nitrogen at pressure of 1–15 Torr.

The discharge was ignited in a metal chamber between the rod powered microwave antenna and a disk grounded electrode. Microwave antenna was a continuation of the central conductor of the coaxial line supplying microwave energy to the chamber. A microwave discharge was created at the end of the antenna. DC voltage was applied between the antenna and the disk electrode. The antenna had a positive potential with respect to the disk electrode.

In the absence of direct current, microwave discharge exists near the tip of antenna and the luminous

area is surrounded by dark space. When applied, DC voltage is sufficient for ignition of DC discharge in the gap with microwave discharge, a glow appears in the area of a grounded disc electrode. Both discharges coexist in the gap creating the hybrid discharge.

Microwave discharge pre-activates the space between the electrodes and facilitates the ignition of DC discharge. Therefore, DC discharge can be attributed to the class of non-self-sustained discharges. It exists in the halo of microwave discharge. Since the properties of microwave discharge are practically independent of the applied DC voltage, changing the characteristics of the microwave discharge provides an independent parameter controlling the properties of the hybrid discharge.

The spectral composition of the discharge radiation near the antenna is represented by bands of the first and second positive systems of nitrogen and weakly depends on DC current. Applied DC voltage is concentrated near the disk electrode, which serves as a cathode in these experiments. The spectral composition of discharge emission in this region is represented by bands of the second positive and first negative nitrogen systems. The intensity of the latter prevails over the intensity of the second positive system with increasing DC current.

Hybrid microwave-DC discharge can be useful for solution of different practical problems of application of low-temperature plasma.

### FUNDING

This work was done as part of TIPS RAS State Plan.

### ADDITIONAL INFORMATION

The article is published in the original.

### REFERENCES

1. Samukawa, S., et al., *J. Phys. D: Appl. Phys.*, 2012, vol. 45, 253001.
2. Bruggeman, P.J., et al., *Plasma Sources Sci. Technol.*, 2016, vol. 25, 053002.
3. Heintz, R.J., *Appl. Phys.*, 1968, vol. 39, p. 1741.
4. Suzuki, K., Okudira, S., Sakudo, N., and Kanomata, I., *Jpn. J. Appl. Phys.*, 1977, vol. 16, p. 1979.
5. Bardos, L., Dragila, R., Lonear, G., and Musil, J., *Rozpr. Cesk. Akad. Ved, Rada Tech. Ved*, 1983, vol. 93, p. 86.
6. Ohkubo, K. and Matsuda, K., *Jpn. J. Appl. Phys.*, 1978, vol. 17, p. 117.
7. *Proc. 8th Int. Symp. Plasma Chem., Special Symp. ECR and Magnetomicrowave Plasma*, Tokyo, Japan, 1987, p. 2399.
8. Musil, J., *Vacuum*, 1986, vol. 36, p. 161.
9. *Microwave Excited Plasmas*, Moisan, M. and Pelletier, J., Eds., Amsterdam: Elsevier, 1992.
10. Klemberg-Sapieha, J.E., Küttel, O.M., and Wertheimer, M.R., *Thin Solid Films*, 1990, vols. 193–194, p. 965.

11. Reinke, P., Bureau, S., Klemberg-Sapieha, J.E., and Martinu, L., *J. Appl. Phys.*, 1994, vol. 78, p. 4855.
12. Ivanov, O.A., Lobaev, M.A., Isaev, V., and Vikharev, A.L., *Phys. Rev. Accel. Beams*, 2010, vol. 13, 022004.
13. Tang, D. and Chu, P.K., *J. Appl. Phys.*, 2003, vol. 93, p. 5883.
14. Frolov, V., Matveev, I., Ivanov, D., Zverev, S., Ushin, B., and Petrov, G., *Rom. J. Phys.*, 2011, vol. 56, no. 1 (suppl.), p. 36.
15. Kuo, S.P., Bivolaru, D., Williams, S., and Carter, C.D., *Plasma Sources Sci. Technol.*, 2006, vol. 15, p. 266.
16. Itarashiki, T., Hayashi, N., and Yonesu, A., *Jpn. J. Appl. Phys.*, 2006, vol. 55, no. 1S, 01AB03.
17. Pearton, S.J., Chakrabarti, U.K., Katz, A., et al., *Plasma Chem. Plasma Process.*, 1991, vol. 11, p. 405.
18. Hala, A.M., Oksuz, L., and Zhu, X., *Plasma Sci. Technol.*, 2016, vol. 18, p. 832.
19. Ayrapetov, A., Kralkina, E., Neklyudova, P., et al., *Nanoindustriya*, 2016, no. 8, p. 104. <http://www.nanoindustry.su/journal/article/en/5795>.
20. Abdali, A., Moritz, B., Gupta, A., et al., *J. Optoelectron. Adv. Mater.*, 2010, vol. 12, p. 440.
21. Lebedev, Yu.A., *Plasma Sources Sci. Technol.*, 2015, vol. 24, 053001.
22. Lebedev, Yu.A., Tatarinov, A.V., and Epshtein, I.L., *High Temp.*, 2007, vol. 45, no. 3, p. 283.
23. Lebedev, Yu.A. and Yusupova, E.V., *Plasma Phys. Rep.*, 2012, vol. 38, no. 8, p. 620.
24. Lebedev, Yu.A., Epstein, I.L., and Yusupova, E.V., *High Temp.*, 2014, vol. 52, no. 2, p. 150.
25. Pearse, R.W.B. and Gaydon, A.G., *The Identification of Molecular Spectra*, London: Chapman and Hall, 1976, 4th ed.
26. Cicala, G., De Tommaso, E., Rain, A.C., et al., *Plasma Sources Sci. Technol.*, 2009, vol. 18, 025032.
27. Lebedev, Yu.A., Tatarinov, A.V., and Epstein, I.L., *Plasma Sources Sci. Technol.*, 2007, vol. 16, p. 726.
28. Lebedev, Yu.A., Solomakhin, P.V., and Shakhatov, V.A., *Plasma Phys. Rep.*, 2007, vol. 33, no. 2, p. 157.
29. Lebedev, Yu.A. and Epstein, I.L., *Plasma Phys. Rep.*, 2007, vol. 33, no. 1, p. 63.
30. Lebedev, Yu.A., Tatarinov, A.V., and Epshtein, I.L., *High Temp.*, 2010, vol. 49, no. 5, p. 775.
31. Bardos, L. and Lebedev, Yu.A., *High Temp.*, 2000, vol. 38, no. 4, p. 528.